Extrema of Two-Port Network Transducer Power Gain and Voltage Gain Under Varying Port Terminations: Semi-Analytical Method and Application to Biotelemetry System

Toni Björninen

BioMediTech Institute and Faculty of Biomedical Sciences and Engineering
Tampere University of Technology, Tampere, 33101, Finland
toni.bjorninen@tut.fi

Abstract ─ Analysis of the structure of the level sets of transducer power gain and voltage gain of a two-port network enables a semi-analytical method for finding the extrema these performance indicators as the port terminations vary in bounded rectangles in the complex plane. In particular, we show that the extrema are necessarily attained in small-dimensional subsets of the given rectangles. This provides efficient means to assess the impact of variability in the port terminations numerically. As an example, we study how variability in the port terminations affects the performance of a biotelemetry system composed of magnetically coupled small loops with highly sensitive impedance matching properties.

Index Terms ─ Sensitivity analysis, tolerance analysis, transducer power gain, two-port networks, voltage gain.

I. INTRODUCTION

Fundamental optimisation approaches aim at maximising the performance of electromagnetic systems in their nominal operating conditions. In two-port microwave networks, which are the focus in this work, a typical goal is the bi-conjugate impedance matching that maximises the power transfer efficiency from the source to the load. This is a relevant goal in virtually all applications, including the recently emerged radio-frequency systems, which operate on harvested energy [1–4]. In such systems, however, also a certain voltage threshold must be exceeded to activate semiconductor devices. This makes the voltage gain another important parameter. A feature shared by both gain parameters in two-port systems is that they are non-linear functions of the complex impedances terminating the ports. Consequently, it is problematic to conclude how variability in the port terminations affect these fundamental performance indicators. In the related previous work, sensitivity of specific two-port networks was characterised through derivative-based approaches [5–6]. In article [7], the authors presented analysis of constant mismatch circles to establish optimum trade-off between input and output mismatch for transistor amplifier design. The authors of [8] investigated the stability of two-port network with terminations varying in elliptic regions in the complex plane. In [4], the minimum of the voltage gain was computed numerically in a special case where the load impedance varied in a disk defined by a given lower bound of the transducer power gain.

In our earlier work [9], we showed that as the port terminations of a two-port network vary in bounded rectangles in the complex plane, the minimisers of the transducer power gain and voltage gain are located necessarily in small-dimensional subsets of the rectangles. In this work, we first summarise the relevant analytical considerations regarding the structure of the level sets of the gain parameters from [9] and then show how this enables identifying the subsets that necessarily contain the maximisers of the gain parameters. This way, we achieve the complete sensitivity analysis of two-port networks. The presented method does not involve differentiation, but is fully based on the analysis of the structure of the level sets of the gain parameters. It provides an efficient computation of the extrema of the gain parameters by restricting the search of both the minimum and maximum in small-dimensional subsets of the given tolerance rectangles. As an example, we apply the method in the analysis of a highly sensitivity biotelemetry system composed of magnetically coupled small loops.

II. LEVEL SETS PF TRANSDUCER POWER GAIN AND VOLTAGE GAIN

Transducer power gain (G_t) of a two-port network is the ratio of the power delivered to the load ($Z_L=R_L+jX_L$) connected to Port 2 of the system to the power available from a Thévenin voltage source with internal impedance of $Z_S=R_S+jX_S$ connected to Port 1. It is given by [10, Ch. 2]:

Submitted On: May 12, 2017
Accepted On: May 21, 2018

$$G_t = \frac{4R_S R_L |z_{21}|^2}{|(Z_S + z_{11})(Z_L + z_{22}) - z_{12}z_{21}|^2}, \quad (1)$$

where z_{mn}, (m=1,2; n=1,2) are the two-port Z-parameters. In this work, only passive port terminations and unconditionally stable systems are considered. In this case we have [10, Ch. 2]:

$$\begin{cases} 0 < R_S \text{ and } 0 < R_L, \\ 0 < \mathrm{Re}(z_{11}) \text{ and } 0 < \mathrm{Re}(z_{22}), \\ |z_{12}z_{21}| < 2\,\mathrm{Re}(z_{11})\mathrm{Re}(z_{22}) - \mathrm{Re}(z_{12}z_{21}), \end{cases} \quad (2)$$

which implies that the input and output impedances given by:

$$Z_i = z_{11} - \frac{z_{12}z_{21}}{z_{22} + Z_L} \text{ and } Z_o = z_{22} - \frac{z_{12}z_{21}}{z_{11} + Z_S}, \quad (3)$$

respectively, have positive real parts.

The voltage gain (A_v) of a two-port system is given by is the ratio of the load (connected to Port 2) voltage amplitude to the amplitude of a Thévenin voltage source with internal impedance of Z_S=R_S+jX_S connected to Port 1. Basic circuit analysis utilising the Z-parameters yield:

$$A_v = \left| \frac{z_{21}Z_L}{(Z_S + z_{11})(Z_L + z_{22}) - z_{12}z_{21}} \right|. \quad (4)$$

A. Level sets of transducer power gain

For further analysis, it is useful to restate Equation (1) as:

$$\begin{cases} G_t = \dfrac{2\Lambda_L R_S}{|Z_S + Z_i|^2}, \quad \Lambda_L = \dfrac{2R_L |z_{21}|^2}{|Z_L + z_{22}|^2}, \\ G_t = \dfrac{2\Lambda_S R_L}{|Z_L + Z_o|^2}, \quad \Lambda_S = \dfrac{2R_S |z_{21}|^2}{|Z_S + z_{11}|^2}. \end{cases} \quad (5)$$

Next, we suppose that Z_S and Z-parameters are fixed and study the condition $\alpha \le G_t(Z_L)$, where $\alpha > 0$. In this case, (5) implies:

$$Z_L Z_L^* + \left(Z_o^* - \frac{\Lambda_S}{\alpha}\right) Z_L + \left(Z_o - \frac{\Lambda_S}{\alpha}\right) Z_L^* + |Z_o|^2 \le 0, \quad (6)$$

which defines a complex plane disk $D_{\alpha L}$ with the centre point ($C_{\alpha L}$) and radius ($r_{\alpha L}$) given by:

$$C_{\alpha L} = -\left(Z_o^* - \frac{\Lambda_S}{\alpha}\right)^* = \frac{\Lambda_S}{\alpha} - Z_o \quad (7)$$

$$\text{and} \quad r_{\alpha L} = \sqrt{|C_{\alpha L}|^2 - |Z_o|^2} = \sqrt{\frac{\Lambda_S}{\alpha}\left(\frac{\Lambda_S}{\alpha} - 2R_o\right)}.$$

Hence, for any Z_S, the load plane level set defined by $\alpha = G_t(Z_L)$ is a circle and $\alpha \le G_t(Z_L)$ holds true in the disk $D_{\alpha L}$ bound by this circle. Analogously we find that for any Z_L, the source plane level set defined by $\alpha = G_t(Z_S)$ is a circle with the centre point ($C_{\alpha S}$) and radius ($r_{\alpha S}$) given by:

$$C_{\alpha S} = \frac{\Lambda_L}{\alpha} - Z_i \quad \text{and} \quad r_{\alpha S} = \sqrt{\frac{\Lambda_L}{\alpha}\left(\frac{\Lambda_L}{\alpha} - 2R_i\right)}, \quad (8)$$

and that $\alpha \le G_t(Z_S)$ holds true in a disk $D_{\alpha S}$ bound by this circle.

By setting the radius to zero in Equations (7)–(8), we find the level sets of $G_t(Z_L)$ and $G_t(Z_S)$ defined by α=Λ_S/(2R_o) and α=Λ_L/(2R_i) to be singletons $\{C_{\alpha L}\}$=$\{Z_o^*\}$ and $\{C_{\alpha S}\}$=$\{Z_i^*\}$, respectively. These special cases correspond to complex-conjugate match at the output and input of the system, respectively, and for a larger α, the level sets are empty. Thus, in the standard terminology of two-port systems, Λ_S/(2R_o) = G_a and Λ_L/(2R_i) = G_p, where G_a and G_p are the available power gain and operating power gain, respectively [10, Ch. 2]. Moreover, (7)–(8) show that the imaginary parts of $C_{\alpha L}$ and $C_{\alpha S}$ are independent of α, whereas their real parts grow monotonically towards infinity as α reduces. At the same time the radii $r_{\alpha L}$ and $r_{\alpha S}$ also tend monotonically towards infinity, but due to the level set property, for any $\alpha_2 < \alpha_1$ we have $D_{\alpha S1} \subset D_{\alpha S2}$ and $D_{\alpha L1} \subset D_{\alpha L2}$. Figure 1 shows an illustration of the level sets of G_t in the source plane.

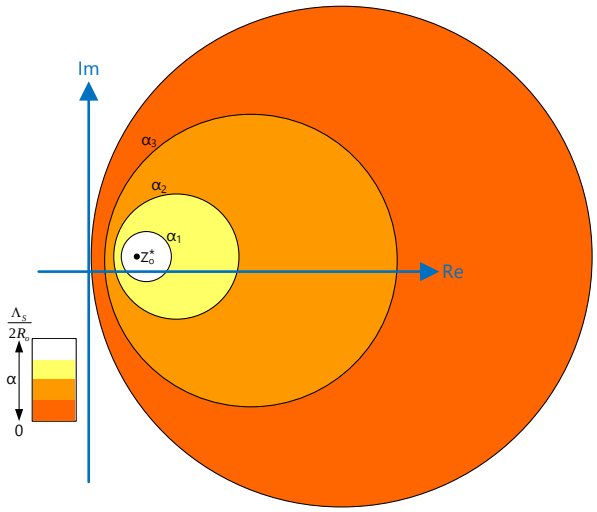

Fig. 1. Illustration of the level sets of G_t in the load plane with $\alpha_1 > \alpha_2 > \alpha_3$ [9].

B. Level sets of voltage gain

First, we note that it is useful to restate Equation (4) as:

$$A_v = \Lambda \left| \frac{Z_L}{Z_L + Z_o} \right|, \quad \Lambda = \left| \frac{z_{21}}{Z_S + z_{11}} \right|. \quad (9)$$

Next, we suppose that Z_L and the Z-parameters are fixed and study the condition $\alpha \le A_v(Z_S)$. In this case, (9) implies:

$$|Z_S - C_{\alpha S}| \le \frac{1}{\alpha} \left| \frac{z_{21}Z_L}{Z_L + z_{22}} \right| = r_{\alpha S}, \; C_{\alpha S} = -Z_i, \quad (10)$$

which defines a disk $D_{\alpha S}$ with the centre point and radius of $C_{\alpha S}$ and $r_{\alpha S}$, respectively. Hence, the level sets defined by $\alpha = A_v(Z_S)$ are circles and $\alpha \le A_v(Z_S)$ holds true in $D_{\alpha S}$.

We suppose next that Z_S and the Z-parameters are fixed and study the condition $\alpha \le A_v(Z_L)$. Now, (10) implies:

$$\mathrm{Z_L Z_L^*} + \frac{\mathrm{Z_o^*}}{\mathrm{P}}\mathrm{Z_L} + \frac{\mathrm{Z_o}}{\mathrm{P}}\mathrm{Z_L^*} + \frac{|\mathrm{Z_o}|^2}{\mathrm{P}} \begin{cases} \le 0, & \mathrm{P} > 0, \\ \ge 0, & \mathrm{P} < 0, \end{cases} \quad (11)$$

where $P = 1-\Lambda^2/\alpha^2$. For $\alpha>\Lambda$, (11) defines a complex plane disk $D_{\alpha L}$ with the centre ($C_{\alpha L}$) and radius ($r_{\alpha L}$) given by:

$$C_{\alpha L} = \frac{-Z_o}{P} \text{ and } r_{\alpha L} = \sqrt{|C_{\alpha L}|^2 - \frac{|Z_o|^2}{P}} = \frac{\Lambda}{\alpha}\left|\frac{Z_o}{P}\right|. \quad (12)$$

For $\alpha<\Lambda$, (11) defines the complex plane excluding $D_{\alpha L}$. Finally, in case $\alpha=\Lambda$, (11) defines a region comprised of the complex plane on and below the line:

$$L_\Lambda = \left\{ x + jy : x = -\frac{X_o}{R_o} y - \frac{|Z_o|^2}{2R_o} \right\}. \quad (13)$$

Figure 3 in Section IV illustrates of the level sets of A_v in the load plane. Finally, the limit processes for the level sets of A_v are summarised as follows:

$$\alpha \to 0 \Rightarrow \begin{cases} r_{aS} \to \infty \text{ and } C_{\alpha S} = -Z_i \\ r_{aL} \to 0 \text{ and } C_{\alpha L} = 0 \end{cases}$$

$$\alpha \uparrow \Lambda \Rightarrow \begin{cases} r_{aL} \to \infty \\ C_{\alpha L} \to \infty \pm j\infty \\ D_{\alpha L} \to \text{Complex plane above } L_\Lambda \end{cases} \quad (14)$$

$$\alpha \downarrow \Lambda \Rightarrow \begin{cases} r_{aL} \to \infty \\ C_{\alpha L} \to -\infty \pm j\infty \\ D_{\alpha L} \to \text{Complex plane below } L_\Lambda \end{cases}$$

$$\alpha \to \infty \Rightarrow \begin{cases} r_{aS} \to 0 \text{ and } C_{\alpha S} \to -Z_i \\ r_{aL} \to 0 \text{ and } C_{\alpha L} \to -Z_o \end{cases}$$

III. EXTREMA OF TRANSDUCER POWER GAIN

In this and the next section, we assume that the port terminations vary in a closed and bounded hyper-rectangle $U = U_S \times U_L$ where U_S and U_L are rectangles in the complex plane given by:

$$\mathrm{U_S} = \left\{ \begin{matrix} \mathrm{x + jy} : 0 < \mathrm{x_{S1}} \le \mathrm{x} \le \mathrm{x_{S2}}, \\ \mathrm{y_{S1}} \le \mathrm{y} \le \mathrm{y_{S2}} \end{matrix} \right\},$$
$$\mathrm{U_L} = \left\{ \begin{matrix} \mathrm{x + jy} : 0 < \mathrm{x_{L1}} \le \mathrm{x} \le \mathrm{x_{L2}}, \\ \mathrm{y_{L1}} \le \mathrm{y} \le \mathrm{y_{L2}} \end{matrix} \right\}. \quad (15)$$

Below, we will detail how the knowledge of the structure of the level sets of G_t and A_v enables the identification of small-dimensional subsets of U where the studied gain parameters necessarily attain their extreme values. To aid the further analysis, we denote the sets of corner and boundary points of U_S and U_L by V_S and V_L, and B_S and B_L, respectively.

Since G_t and A_v are continuous real-valued functions which can also be interpreted as functions of four real variables in a closed and bounded set defined by the intervals of the real and imaginary parts in Equation (15), Extreme Value Theorem guarantees that they attain their extreme values in U [11, Ch. 12.5].

B. Minimum of transducer power gain

The level sets of G_t are circles in both the source and load planes. We focus first on the source plane, where $\alpha \le G_t(Z_S)$ holds true in a disk $D_{\alpha S}$ which is bound by the level set circle. Hence, to bound $G_t(Z_S)$ from below in U_S, we must find the smallest α for which U_S is entirely contained in $D_{\alpha S}$. Since U_S is a rectangle, such α defines a level set circle that passes through a corner of U_S. Hence, for all Z_S in U_S we have $G_t(Z_S) \ge G_t(Z_{S0})$, where $Z_{S0} \in V_S$. With a similar reasoning, for all Z_L in U_L, we have $G_t(Z_L) \ge G_t(Z_{L0})$, where $Z_{L0} \in V_L$. Consequently, for all (Z_S,Z_L) in U: $G_t(Z_S,Z_L) \ge G_t(Z_{S0},Z_L) \ge G_t(Z_{S0},Z_{L0})$. Because this lower bound of G_t over the whole closed and bounded set U is its value evaluated at $(Z_{S0},Z_{L0}) \in U$, then by the Extreme Value Theorem, this point must be the minimiser of G_t in U.

C. Maximum of transducer power gain

For an unconditionally stable two-port, the unique bi-conjugate-matched source and load terminations Z_{mS} and Z_{mL}, respectively, maximise the transducer power gain and the maximum can be computed with the well-known formula [10, Ch. 2]. Clearly, if $(Z_{mS},Z_{mL}) \in U$, this point is the maximiser of G_t in U. Therefore, below we will assume that $(Z_{mS},Z_{mL}) \notin U$. For further analysis, we denote the images of U_L and U_S under the complex conjugate map of the input and output impedances as $Z_i^*[U_L]$ and $Z_o^*[U_S]$, respectively, and make the following definitions: $\Sigma_S = U_S \cap Z_i^*[U_L]$ and $\Sigma_L = U_L \cap Z_o^*[U_S]$.

If Σ_S and Σ_L are both empty, then for an increasing level sets values, the level set circles of G_t must converge towards points outside of U_S and U_L, because neither the input or output can be conjugate-matched. Hence, to bound $G_t(Z_S,Z_S)$ from above in U_S, we must find the largest level set value α for which $D_{\alpha S}$ intersects U_S at a single point only. Such α defines a level set circle that passes through a point in the boundary of U_S. Hence, for all Z_L in U_L, we have $G_t(Z_S,Z_L) \le G_t(Z_{S0},Z_L)$, where $Z_{S0} \in B_S$. With an identical argument, for any $Z_S \in U_S$, we have $G_t(Z_S,Z_L) \le G_t(Z_S,Z_{L0})$, where $Z_{L0} \in B_L$. Consequently, for all (Z_S,Z_L) in U: $G_t(Z_S,Z_L) \le G_t(Z_{S0},Z_L) \le G_t(Z_{S0},Z_{L0})$. Because this upper bound of G_t over the whole closed and bounded set U is its value evaluated at $(Z_{S0},Z_{L0}) \in U$, by the Extreme Value Theorem, this point must be the maximiser of G_t in U.

If either Σ_S or Σ_L or both are non-empty, the maximiser of G_t may be located in the interior of U. To aid the analysis in these cases, we first study the algebraic properties of the map Z_i^* defined as the complex conjugate of the input impedance. Firstly, Z_i^* is clearly continuous in U_L since $\mathrm{Re}(z_{22})$ and R_L are both positive (Equation 2) and thus $z_{22}+Z_L \neq 0$ in Equation (3).

Moreover, it is elementary to show that Z_i^* is injective and thus bijective from its domain to its image. Finally, Equation (3) can be readily solved for Z_L to see that the inverse map Z_i^{*-1} exists and is continuous. These properties make Z_i^* a homeomorphism from U_L to its image. This class of functions map interior and boundary points of their domain to the respective points of the image. Moreover, simply-connectedness is a property that is preserved under a homeomorphic map. Therefore, as the closed and bounded rectangle U_L is clearly simply-connected, so must be the set $Z_i^*[U_L]$.

With analogous arguments as for the map Z_i^*, we find that Z_i^{*-1} is a homeomorphism from Σ_S to its image $Z_i^{*-1}[\Sigma_S]$ and thus this set must be simply-connected and its boundary given by $Z_i^{*-1}[\partial\Sigma_S]$, where $\partial\Sigma_S$ denotes the boundary of Σ_S. Since Z_i^* and Z_o^* have identical structure, all of the above conclusions are true for Z_o^* and its inverse as well. Finally, we note that since we have assumed that the bi-conjugate-matched source and load impedances of the two-port system are not located in U, we must have $\Sigma_S \cap Z_o^{*-1}[\Sigma_L] = \emptyset$ and $\Sigma_L \cap Z_i^{*-1}[\Sigma_S] = \emptyset$.

Next, we suppose Σ_S is non-empty. This implies that there exists $Z_{L1} \in Z_i^{*-1}[\Sigma_S]$ such that $Z_i^*(Z_{L1}) = Z_{S1} \in \Sigma_S$. In general, $G_t(Z_S,Z_L) \le G_p(Z_L)$, where G_p is the operating power gain of the two-port network attained when the input is conjugate-matched. Because the input is conjugate-matched at the point (Z_{S1},Z_{L1}), G_t attains its upper bound $G_p(Z_L)$ w.r.t. the source impedance at this point. However, since $\Sigma_L \cap Z_i^{*-1}[\Sigma_S] = \emptyset$, the level sets of G_t in the load plane converge towards a point outside of $Z_i^{*-1}[\Sigma_S]$. Hence, to bound G_t from above in $\Sigma_S \times Z_i^{*-1}[\Sigma_S]$, we must find the largest α for which $D_{\alpha L}$ intersects $Z_i^{*-1}[\Sigma_S]$ at a single point only. Such α defines a level set circle that passes through a point in the boundary of $Z_i^{*-1}[\Sigma_S]$. Thus, for all $(Z_S,Z_L) \in \Sigma_S \times Z_i^{*-1}[\Sigma_S]$, we have $G_t(Z_S,Z_L) \le G_t(Z_{S1},Z_{L1})$, where $Z_{L1} \in Z_i^{*-1}[\partial\Sigma_S]$ and $Z_{S1} = Z_i^*(Z_{L1})$.

In case Σ_L is non-empty, then by identical arguments as above, we have $G_t(Z_S,Z_L) \le G_a(Z_S)$, where G_a is the available power gain of the two-port network attained when the output is conjugate-matched and we conclude that for all $(Z_S,Z_L) \in Z_o^{*-1}[\Sigma_L] \times \Sigma_L$ we have $G_t(Z_S,Z_L) \le G_t(Z_{S2},Z_{L2})$, where $Z_{S2} \in Z_o^{*-1}[\partial\Sigma_L]$, $Z_{L2} = Z_o^*(Z_{S2})$.

Finally, since $\Sigma_S \times Z_i^{*-1}[\Sigma_S]$ and $\Sigma_L \times Z_o^{*-1}[\Sigma_L]$ are proper subsets of U, the upper bound of G_t in the whole U may be larger than $\max\{G_t(Z_{S1},Z_{L1}),\ G_t(Z_{S2},Z_{L2})\}$. However, for a level set value α that is strictly greater than this value, the level sets of G_t are either empty, if (Z_{S1},Z_{L1}) or (Z_{S2},Z_{L2}) happens to be the maximiser of G_t in U, or converge towards points outside of U_S and U_L. This is because, in all cases where level sets convergence towards a point inside U_S or U_L, G_t is upper bounded by $\max\{G_t(Z_{S1},Z_{L1}), G_t(Z_{S2},Z_{L2})\} < \alpha$ as shown above. Thus, for all (Z_S,Z_L) in U, we have $G_t(Z_S,Z_L) \le \max\{G_t(Z_{S0},Z_{L0}), G_t(Z_{S1},Z_{L1}), G_t(Z_{S2},Z_{L2})\}$, where $(Z_{S0},Z_{L0}) \in B_S \times B_L$.

Based on these findings, we conclude that the maximiser of G_t in U is necessarily located in a small-dimensional subset of U as summarised below. Figure 2 illustrates the search of the maximiser of G_t in U_L in case (d) of the below list.

(a) If $(Z_{mS},Z_{mL}) \in U$, the maximum of G_t in U is $G_t(Z_{mS},Z_{mL})$.

(b) If $\Sigma_S = \emptyset$ and $\Sigma_L = \emptyset$, the maximiser of G_t in U is a point $(Z_{S0},Z_{L0}) \in B_S \times B_L$.

(c) If $\Sigma_S \neq \emptyset$ and $\Sigma_L = \emptyset$, the maximiser of G_t in U is (Z_{S0},Z_{L0}) or a point (Z_{S1},Z_{L1}), where $Z_{L1} \in Z_i^{*-1}[\partial\Sigma_S]$ and $Z_{S1} = Z_i^*(Z_{L1})$.

(d) If $\Sigma_S = \emptyset$ and $\Sigma_L \neq \emptyset$, the maximiser of G_t in U is (Z_{S0},Z_{L0}) or a point (Z_{S2},Z_{L2}), where $Z_{S2} \in Z_o^{*-1}[\partial\Sigma_L]$ and $Z_{L2} = Z_o^*(Z_{S2})$.

(e) If $\Sigma_S \neq \emptyset$ and $\Sigma \neq \emptyset$, the maximiser of G_t in U is (Z_{S0},Z_{L0}), (Z_{S1},Z_{L1}) or (Z_{S2},Z_{L2}).

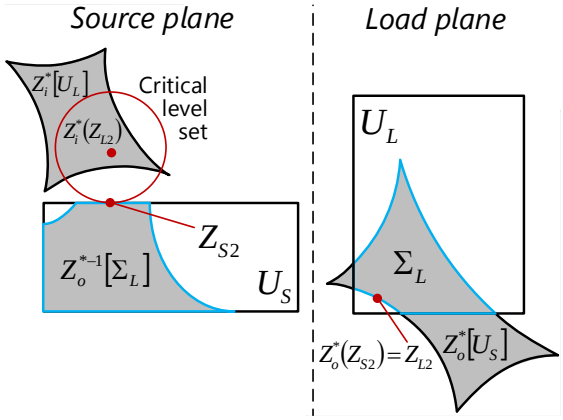

Fig. 2. Illustration of the search of maximiser of G_t in U in the case $\Sigma_S = \emptyset$ and $\Sigma_L \neq \emptyset$. The figure has been drawn supposing the maximiser is (Z_{S2},Z_{L2}).

IV. EXTREMA OF VOLTAGE GAIN

A. Minimum of voltage gain

In the source plane, the level sets defined by $\alpha=A_v(Z_S)$ are circles given in Equation (9) and $\alpha \le A_v(Z_S)$ holds true in a disk $D_{\alpha S}$ which is bound by the level set circle. Hence, to bound $A_v(Z_S)$ from below in U_S, we must find the smallest α for which U_S is contained in $D_{\alpha S}$. Since U_S is a rectangle, such α defines a level set circle which passes through a corner of U_S. As seen from Equation (9), the centre point of the level set circle has a negative real part and the circle radius is inversely proportional to α. Therefore, since every point in U_S has a positive real part, the set of possible corners of intersection are limited to those with larger real parts. We denote these corners as $V_{S+}=\{x_{S2}+jy_{S1}, x_{S2}+jy_{S2}\}$. Hence, for all Z_S in U_S we have $A_v(Z_S) \ge A_v(Z_{S0})$, where $Z_{S0} \in V_{S+}$.

To bound $A_v(Z_L)$ from below in U_L, we first suppose that the minimum of $A_v(Z_L)$ in V_L is attained at a point

Z_{L1}. If $A_v(Z_{L1})>\Lambda$, then the level set circle that passes through Z_{L1} must be the boundary of a disk $D_{\alpha L}$ where $A_v(Z_L)\geq A_v(Z_{L1})$. Given that Z_{L1} is a corner point of U_L and minimises $A_v(Z_L)$ in V_L, then the remaining corners of U_L must be contained in $D_{\alpha L}$. Since U_L is a rectangle, this implies that U_L must be entirely contained $D_{\alpha L}$. Thus, $A_v(Z_L)\geq A_v(Z_{L1})$ for all Z_L in U_L.

If $A_v(Z_{L1})<\Lambda$, there may be more points in U_L for which A_v is smaller than $A_v(Z_{L1})$. For any such point Z_{L2}, $A_v(Z_L)\geq A_v(Z_{L2})$ holds true outside of $D_{\alpha L}$ with the corresponding level set circle passing through Z_{L2}. Thus, to bound $A_v(Z_L)$ from below in U_L, we must find the smallest α such that $D_{\alpha L}$ intersects U_L at a single point only. Based on the limit processes summarised in Equation (14), as α reduces from Λ towards 0, then $C_{\alpha L}\to 0$ and $r_{\alpha L}\to 0$. However, by the definition of U_L given in Equation (15), $0\notin U_L$. Thus, the intersection point must be found in B_L.

By combining the results from the above discussion, since $V_L\subset B_L$, for all (Z_S,Z_L) in U we have $A_v(Z_S,Z_L)\geq A_v(Z_{S0},Z_L)\geq A_v(Z_{S0},Z_{L0})$, where $(Z_{S0},Z_{L0})\in V_{S+}\times B_L$. Because this lower bound of A_v over the whole closed and bounded set U is its value evaluated at $(Z_{S0},Z_{L0})\in U$, then by the Extreme Value Theorem, this point must be the minimiser of A_v in U. Figure 3 illustrates the search of the minimiser of A_v in U_L.

B. Maximum of voltage gain

In the source plane, the level sets defined by $\alpha=A_v(Z_S)$ are circles given in Equation (9) and $\alpha\leq A_v(Z_S)$ holds true in a disk $D_{\alpha S}$ which is bound by the level set circle. Hence, to bound $A_v(Z_S)$ from above in U_S, we must find the largest α for which $D_{\alpha S}$ intersects U_S only at a single point. Since U_S is a rectangle, such α defines a level set circle that passes through a point at the boundary of U_S. As seen from Equation (9), the centre point of the level set circle has a negative real part and the circle radius is inversely proportional to α. Therefore, since every point in U_S has a positive real part, the intersection point must lie on the vertical edge of U_S with the smaller real part. We denote this set as $B_{S-}=\{x+jy: x=x_{S1},\ y_{S1}\leq y\leq y_{S2}\}$. Hence, for all Z_S in U_S we have $A_v(Z_S)\leq A_v(Z_{S0})$, where $Z_{S0}\in B_{S-}$.

To bound $A_v(Z_L)$ from above in U_L, we first suppose that the maximum of $A_v(Z_L)$ in V_L is attained at a point Z_{L1}. If $A_v(Z_{L1})<\Lambda$, the level set circle passing through Z_{L1} defines a disk $D_{\alpha L}$ where $A_v(Z_L)<A_v(Z_{L1})$. Given that Z_{L1} is a corner point of U_L and maximises $A_v(Z_L)$ in V_L, the remaining corners must be contained in $D_{\alpha L}$. Since U_L is a rectangle, this implies that U_L must be entirely contained in $D_{\alpha L}$. Thus, $A_v(Z_L)<A_v(Z_{L1})$ for all Z_L in U_L.

If $A_v(Z_{L1})>\Lambda$, there may be more points in U_L for which A_v is greater than $A_v(Z_{L1})$. For any such point Z_{L2}, $A_v(Z_L)\leq A_v(Z_{L2})$ holds true outside of $D_{\alpha L}$ with the corresponding level set circle passing through Z_{L2}. Thus, to bound $A_v(Z_L)$ from above in U_L, we must find the largest α such that $D_{\alpha L}$ intersects U_L at a single point only. Based on the limit processes summarised in Equation (14), as α grows from Λ towards infinity, $C_{\alpha L}\to 0$ and $r_{\alpha L}\to 0$. By the definition of U_L given in Equation (15), $0\notin U_L$. Thus, the intersection point must be found in B_L.

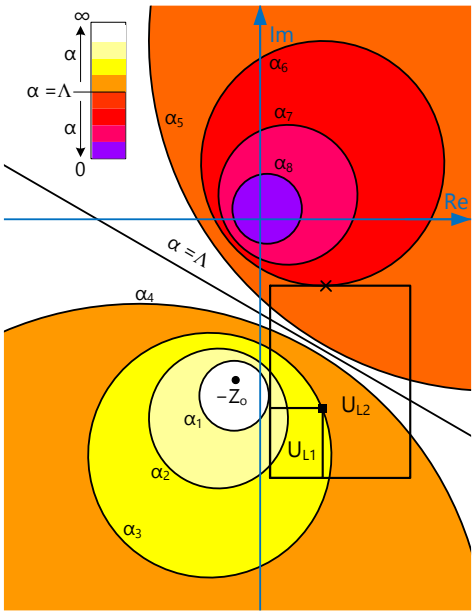

Fig. 3. Illustration of the search of minimiser of A_v in the load plane in rectangles U_{L1} and U_{L2}. In the figure: $\alpha_n > \alpha_{n+1}$ and $\alpha_4>\Lambda>\alpha_5$. The box and cross markers indicate the minimiser of A_v in U_{L1} and U_{L2}, respectively [9].

By combining the results from the above discussion, since $V_L\subset B_L$, for all (Z_S,Z_L) in U we have $A_v(Z_S,Z_L)\leq A_v(Z_{S0},Z_L)\leq A_v(Z_{S0},Z_{L0})$, where $(Z_{S0},Z_{L0})\in B_{S-}\times B_L$. Because this upper bound of A_v over the whole closed and bounded set U is its value evaluated at $(Z_{S0},Z_{L0})\in U$, then by the Extreme Value Theorem, this point must be the minimiser of A_v in U.

In practice, the search for the maximiser of A_v in U is initialised by finding the maximiser (Z_{S0},Z_{L1}) of A_v in $B_{S-}\times V_L$. This is readily done, since this is a small subset of U. Next Λ given in Equation (9) is computed at $Z_S=Z_{S0}$. If $A_v(Z_{S0},Z_{L1})<\Lambda$, then (Z_{S0},Z_{L1}) maximises A_v in U. Otherwise, the maximum value is attained in $B_{S+}\times B_L$ which is also a limited subset of U. The search for the minimiser follows an analogous algorithm.

V. APPLICATION TO ANALYSIS OF A BIOTELEMETRY SYSTEM

The presented technique of finding the extrema of the transducer power gain and voltage gain of a two-port network as the source and load impedances vary in given rectangles in the complex plane is applicable to all two-ports which are unconditionally stable. In this section, we present an example in the analysis of a wireless link

in a biotelemetry system.

We consider a wireless link between a miniature loop antenna formed by metallizing four adjacent faces of a 1×1×1 mm^3 sized cube and a planar circular loop with the inner diameter of 12 mm, which has been developed for a wireless brain-machine interface system [3]. In this application, the cubic loop lies on the cortex harvesting energy for a microsystem that records the electrical activity of the brain. The source of energy is a planar loop placed 5 mm above the scalp transmitting at 300 MHz. A major practical challenge in the implementation and testing of the wireless link is the impedance matching of the small loops. This is because they have very low input resistance and consequently the system is sensitive towards variability in the antenna terminations.

For testing the wireless link, the antennas need to be matched to 50 Ω instruments. To bi-conjugate match the system, we computed the unique matched source and load terminations to achieve this and implement matching circuits comprised of two reactive components for both antennas. This is a generally applicable approach to transform any complex impedance to a given resistance [12, Ch. 5.1]. In this process, we utilised the simulated Z-parameters of the wireless link including the antennas and biological channel that we obtained from simulations in ANSYS HFSS as detailed in [3]. As shown in [3], due to the miniature size of the implanted antenna and the biological environment, the maximum link power efficiency in this system is attained around 300 MHz. At this frequency, the component values to realize the bi-conjugate matching were found to be: C_{in} = 13.0 pF, L_{in} = 1.80 nH, C_{out} = 182 pF, and L_{out} = 0.75 nH, where the capacitors are connected in series with the external and implant antennas and followed by the inductors in parallel. At 300 MHz these circuits transform 50 Ω to the matched source and load impedances Z_{mS}=0.695−j63.616 Ω and Z_{mL}=0.049−j2.489 Ω terminating the implant and external antenna ports, respectively. This means that under ideal conditions the system is bi-conjugate matched at 300 MHz with no impedance mismatch loss.

For the assessment of impact of variability in the antenna terminations, the bounds of impedance variation can be defined in numerous ways. We first considered the tolerance rectangles U_S and U_L to be the largest squares centred at Z_{mS} and Z_{mL}, such that the minimum of G_t at 300 MHz was 3 dB (Case 1a) and 6 dB (Case 2a) below the nominal value. As the presented analysis method is applicable to any rectangle, we then extended the squares to largest rectangles so that the drop in G_t from the nominal value remained at 3 dB (Case 1b) and 6 dB (Case 2b) at 300 MHz. Given that the level sets of G_t are circles with the properties detailed in Section II, this can be understood as an extension of the rectangles until the critical level set circle passes through not only one, but at least two of the corners of the tolerance rectangles. Finally, at other frequencies, U_S and U_L were defined through corner points having the same percentage difference in real and imaginary parts with respect to Z_S and Z_L, as in the case at 300 MHz. Table 1 lists the percentage differences defining the rectangles. Table 2 shows the corner points of the rectangles at 300 MHz. Figures 4 and 5 present the simulated transducer power gain and voltage gain of the system together with the bounds of variation given by the impedance tolerance defined in Table 1.

Table 1: Percentage variation in the source and load impedance for the computation of the minimum and maximum of G_t and A_v in Fig. 4

Case 1a			
Re(Z_S)	Im(Z_S)	Re(Z_L)	Im(Z_L)
±1.17%	±1.17%	±1.17%	±1.17%
Case 1b			
Re(Z_S)	Im(Z_S)	Re(Z_L)	Im(Z_L)
–1.17% +364%	±1.17%	–1.29% +21.1%	–1.21% +1.18%
Case 2a			
Re(Z_S)	Im(Z_S)	Re(Z_L)	Im(Z_L)
±1.94%	±1.94%	±1.94%	±1.94%
Case 2b			
Re(Z_S)	Im(Z_S)	Re(Z_L)	Im(Z_L)
–2.24% +1013%	±1.94%	–1.96% +55.1%	–1.95% +1.94%

Table 2: Corner points of the tolerance rectangles (unit: Ω) at 300 MHz for the computation of the minimum and maximum of G_t and A_v in Fig. 4

Case 1a				
U_S	0.228 −j37.72	0.228 −j36.85	0.233 −j37.72	0.233 −j36.85
U_L	0.039 −j1.517	0.039 −j1.482	0.0404 −j1.517	0.0404 −j1.482
Case 1b				
U_S	0.228 −j37.72	0.228 −j36.85	1.07 −j36.85	1.07 −j36.13
U_L	0.039 −j1.518	0.039 −j1.482	0.0483 −j1.518	0.0483 −j1.482
Case 2a				
U_S	0.226 −j38.0	0.226 −j36.56	0.235 −j38.0	0.235 −j36.56
U_L	0.0391 −j1.529	0.0391 −j1.471	0.0407 −j1.529	0.0407 −j1.471
Case 2b				
U_S	0.225 −j38.0	0.225 −j36.56	2.564 −j38.0	2.564 −j36.56
U_L	0.0391 −j1.529	0.0391 −j1.471	0.0619 −j1.529	0.0619 −j1.471

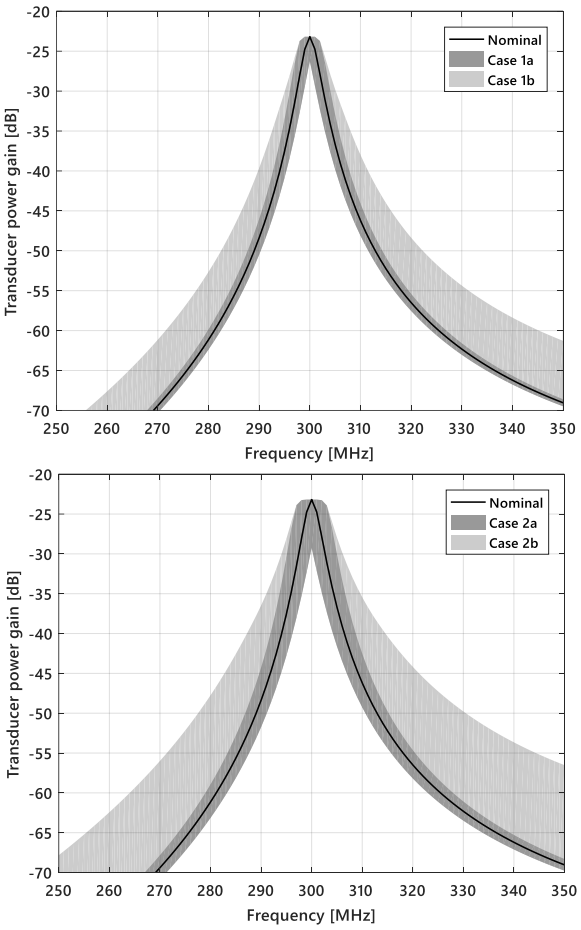

Fig. 4. Transducer power gain of the biotelemetry system and the bounds of variation as the source and load impedances vary in the tolerance rectangles given in Table 1.

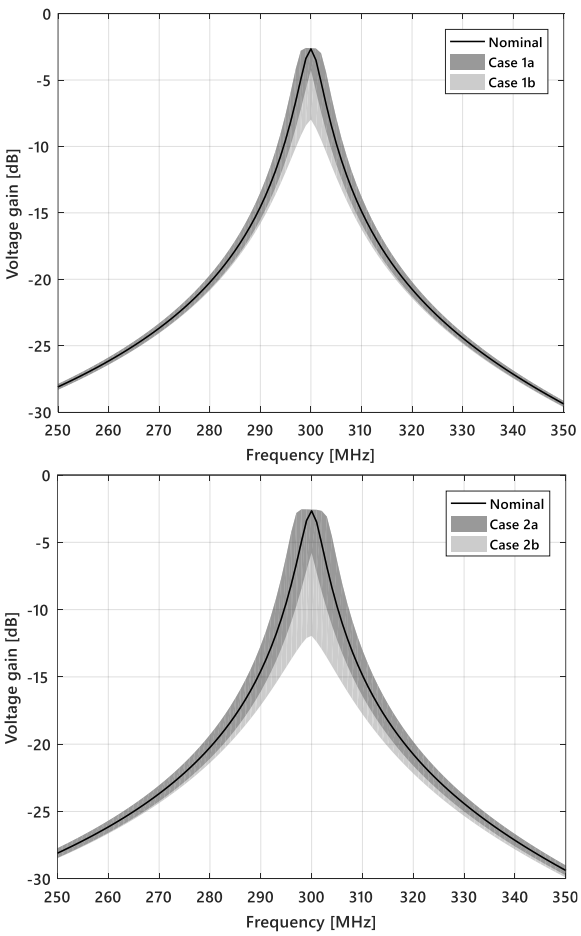

Fig. 5. Voltage gain of the biotelemetry system and the bounds of variation as the source and load impedances vary in the tolerance rectangles given in Table 1.

As seen from Tables 1 and 2, the bounds of variability which correspond to the notable reductions of 3 dB (Case 1) and 6 dB in the transducer power gain compared to the nominal operating conditions, are small. The same conclusion applies to voltage gain, which drops 1.6 dB and 5.3 dB in Case 1a and Case 1b, respectively, and 3.1 dB and 9.3 dB in Case 2a and Case 2b, respectively, at 300 MHz. Overall, it is clear from the results that in this system very small variations in the order of 1-to-2% in the antenna terminations may result in significant reduction in the system's performance. In contrast, however, it tolerates marked deviations in the source and load resistances, towards values higher than the nominal as exemplified by Cases 1b and 2b.

VI. CONCLUSION

Prediction of the performance bounds of electromagnetic systems under non-ideal operating conditions is an important step in achieving reliable devices and conducting reproducible experiments. To aid this process in the context of two-port networks, we developed a semi-analytical method for locating the minimiser and maximiser of the transducer power gain and voltage gain as the port terminations vary in bounded rectangles in the complex plane. Instead of differentiation, the method exploits the knowledge on the structure of the level sets of the gain parameters to limit the numerical search to small-dimensional subsets of the full four-dimension search space. We applied the method in the analysis of a highly sensitive biotelemetry system based

on magnetically coupled small loops. Future work includes comparison of matching circuits to reduce the sensitivity in this type of wireless systems.

ACKNOWLEDGMENT

This research was funded by Academy of Finland funding decision 294616.

REFERENCES

[1] J. Kimionis, M. Isakov, B. S. Koh, A. Georgiadis, and M. M. Tentzeris, "3D-printed origami packaging with inkjet-printed antennas for RF harvesting sensors," *IEEE Trans. Microw. Theory Techn.*, vol. 63, no. 12, pp. 4521-4532, Dec. 2015.

[2] M. Zargham and P. G. Gulak, "Fully integrated on-chip coil in 0.13 µm CMOS for wireless power transfer through biological media," *IEEE Trans. Biomed. Circuits Syst.*, vol. 9, no. 2, pp. 259-271, Apr. 2015.

[3] E. Moradi, S. Amendola, T. Björninen, L. Sydänheimo, J. M. Carmena, J. M. Rabaey, and L. Ukkonen, "Backscattering neural tags for wireless brain-machine interface system," *IEEE Trans. Antennas. Propag.*, vol. 62, no. 2, pp. 719-726, Dec. 2014.

[4] M. Waqas, A. Khan, T. Björninen, L. Sydänheimo, and L. Ukkonen, "Characterization of two-turns external loop antenna with magnetic core for efficient wireless powering of cortical implants," *IEEE Antennas Wireless Propag. Lett.*, vol. 15, pp. 1410-1413, Dec. 2015.

[5] G. I. Vasilescu and T. Redon, "A new approach to sensitivity computation of microwave circuits," *IEEE Intl. Symp. Circuits and Systems*, Espoo, Finland, pp. 1167-1170, June 1988.

[6] F. Güneş and S. Altunç, "Gain-sensitivity analysis for cascaded two-ports and application to distributed-parameter amplifiers," *Intl. J. RF and Microw. Computer-Aided Eng*., vol. 14, no. 5, pp. 462-474, Sep. 2004.

[7] W. Ciccognani, P. E. Longhi, S. Colangeli, and E. Limiti, "Constant mismatch circles and application to low-noise microwave amplifier design," *IEEE Trans. Microw. Theory Techn.*, vol. 61, no. 12, pp. 4154-4167, Dec. 2013.

[8] P. Marietti, G. Scotti, A. Trifiletti, and G. Viviani, "Stability criterion for two-port network with input and output terminations varying in elliptic regions," *IEEE Trans. Microw. Theory Techn.*, vol. 54, no. 12, pp. 4049-4055, Dec. 2006.

[9] T. Björninen, E. Moradi, M. Waqas, A. Khan, and L. Ukkonen, "Minimum of two-port voltage and power gain under varying terminations: Semi-analytic method and application to biotelemetry systems," *URSI Commission B Intl. Symp. On Electromagnetic Theory*, Espoo, Finland, pp. 869-872, Aug. 2016.

[10] Ralph S. Carson, *High-Frequency Amplifiers*. John Wiley & Sons, USA, 1975.

[11] Patrick M. Fitzpatrick, *Advanced Calculus*. 2nd ed., Thomson Brooks/Cole, USA, 2006.

[12] David M. Pozar, *Microwave Engineering*. 4th ed., John Wiley & Sons, Inc., USA, 2012.

Toni Björninen received the M.Sc. and doctoral degrees in Electrical Engineering in 2009 and 2012, respectively, from Tampere University of Technology (TUT), Tampere, Finland. He is currently an Academy of Finland Research Fellow in BioMediTech Institute and Faculty of Biomedical Sciences and Engineering in TUT. He has been a Visiting Postdoctoral Scholar in Berkeley Wireless Research Center in UC Berkeley and in Microwave and Antenna Institute in Electronic Engineering Dept., Tsinghua University, Beijing. His research focuses on technology for wireless health including implantable and wearable antennas and sensors, and RFID-inspired wireless solutions. Björninen is an author of 140 peer-reviewed scientific publications. He serves as an Associate Editor in IET Electronics Letters and IEEE Journal of Radio Frequency Identification, and as an Editor in International Journal of Antennas and Propagation. In 2016, IEEE Antennas and Propagation Society selected him among the top 10 Reviewers of IEEE Transactions on Antennas and Propagation for his input during 06/2015–04/2016.